Neurobiology of Disease 196 (2024) 106521

Contents lists available at ScienceDirect

Neurobiology of Disease

journal homepage: www.elsevier.com/locate/ynbdi

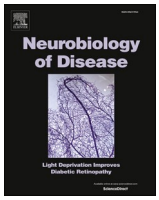

Indirect functional connectivity does not predict overall survival in glioblastoma

Lorenzo Pini [a], Giuseppe Lombardi [b], Giulio Sansone [c], Matteo Gaiola [c], Marta Padovan [b], Francesco Volpin [d], Luca Denaro [c], Maurizio Corbetta [a,c,e,1], Alessandro Salvalaggio [c,*,1]

[a] Padova Neuroscience Center, University of Padova, Italy
[b] Department of Oncology, Oncology 1, Veneto Institute of Oncology IOV-IRCCS, Padova, Italy
[c] Departments of Neuroscience, University of Padova, Italy
[d] Division of Neurosurgery, Azienda Ospedaliera Università di Padova, Padova, Italy
[e] Veneto institute of Molecular Medicine (VIMM), Padova, Italy

ARTICLE INFO

Keywords:
Glioblastoma
Disconnections
Functional imaging
Survival prediction

ABSTRACT

Background: Lesion network mapping (LNM) is a popular framework to assess clinical syndromes following brain injury. The classical approach involves embedding lesions from patients into a normative functional connectome and using the corresponding functional maps as proxies for disconnections. However, previous studies indicated limited predictive power of this approach in behavioral deficits. We hypothesized similarly low predictiveness for overall survival (OS) in glioblastoma (GBM).

Methods: A retrospective dataset of patients with GBM was included ($n = 99$). Lesion masks were registered in the normative space to compute disconnectivity maps. The brain functional normative connectome consisted in data from 173 healthy subjects obtained from the Human Connectome Project. A modified version of the LNM was then applied to core regions of GBM masks. Linear regression, classification, and principal component (PCA) analyses were conducted to explore the relationship between disconnectivity and OS. OS was considered both as continuous and categorical (low, intermediate, and high survival) variable.

Results: The results revealed no significant associations between OS and network disconnection strength when analyzed at both voxel-wise and classification levels. Moreover, patients stratified into different OS groups did not exhibit significant differences in network connectivity patterns. The spatial similarity among the first PCA of network maps for each OS group suggested a lack of distinctive network patterns associated with survival duration.

Conclusions: Compared with indirect structural measures, functional indirect mapping does not provide significant predictive power for OS in patients with GBM. These findings are consistent with previous research that demonstrated the limitations of indirect functional measures in predicting clinical outcomes, underscoring the need for more comprehensive methodologies and a deeper understanding of the factors influencing clinical outcomes in this challenging disease.

1. Introduction

Glioblastoma (GBM) is a rare and highly aggressive form of brain tumor, associated with a grim prognosis. With a median overall survival (OS) rate of approximately fifteen months, it stands as one of the most challenging and devastating malignancies. Despite advances in the understanding of tumors and their treatment, this disease continues to pose a clinical challenge due to the limited success of available interventions (Tan et al., 2020). The complexity of the disease, its rapid progression, and its tendency to infiltrate healthy brain tissue make it difficult to treat. Moreover, the blood-brain barrier and the inherent molecular heterogeneity of glioblastomas contribute to the resistance often seen in conventional therapies (Pandit et al., 2020). Current treatment approaches typically involve a combination of surgery, radiation therapy, and chemotherapy, but even with these aggressive measures, the survival rates remain low (Gilbert et al., 2013; Lin et al., 2021; Stupp et al.,

* Corresponding author.
E-mail address: alessandro.salvalaggio@unipd.it (A. Salvalaggio).
[1] These authors contributed equally to this work and share senior authorship.

https://doi.org/10.1016/j.nbd.2024.106521
Received 28 February 2024; Received in revised form 14 April 2024; Accepted 29 April 2024
Available online 30 April 2024

2009).

While the exact cause of glioblastoma remains elusive, age, extension of the surgery, molecular signature of the tumor, and the performance status are currently used in clinical practice as prognostic factors and in clinical trial as confounding factors for testing disease modifiers (Illic et al., 2017; Mansouri et al., 2020; Ostrom et al., 2018). Notably, these factors do not consider directly the host where all of this occurs, namely the brain.

Nonetheless, it's essential to recognize that the brain is a remarkably intricate organ, and this complexity manifests itself at various levels. This spectrum of complexity ranges from the micro-scale, (i.e., the interactions among different types of cells (neurons and glia) and the intricate network of neurotransmitters), passing through the mesoscale, (the interactions within neural circuits involving around 50.000 neurons which roughly corresponds to 6.000 synapses), to the macroscale layer, assessing how large neural populations communicate via polysynaptic mechanisms and structural connections. Techniques such as functional magnetic resonance imaging (fMRI) and diffusion-weighted imaging (DWI) enable us to explore the connective architecture of the brain and how various neurological disorders affect this intricate organization (Sporns, 2013).

In the last decades, numerous studies have explored how molecular pathologies associated with degenerative conditions (e.g., amyloid-beta, tau, alpha-synuclein, huntingtin) can propagate through this neural connectome. This research highlights a close interplay between the micro-level and macro-level elements of the brain (Buckner et al., 2005; Palmqvist et al., 2017; Pereira et al., 2019; Pini et al., 2020; Warren et al., 2012).

Recent investigations have extended this concept to brain tumors. Mandal et al. have shown that functional hub regions within the brain are susceptible to glioma concentration. Notably, gliomas exhibit a predilection for brain areas expected to act as connector hubs, which facilitate communication between diverse cognitive subsystems, as opposed to local/provincial hubs that primarily handle communication within their respective subsystems (Mandal et al., 2023). These macroscale findings align with molecular insights, as demonstrated by Osswald and colleagues, who uncovered interconnections among GBM cells, enabling the exchange of genetic material and information. This interconnected network augments the tumor's resilience and resistance to conventional cancer treatments like chemotherapy (Osswald et al., 2015), consequently resulting in a more adverse prognosis. Accordingly, intra-network functional connectivity strength within GBM tumors appears to correlate with OS, even after accounting for potential confounding variables (Daniel et al., 2021).

Overall, these findings underscore a strong relationship between OS and the connectivity properties of the brain when assessed directly using patients' data. A novel connectivity framework called lesion network mapping (LNM) has been introduced. The main advantage of LNM is the possibility to estimate the functional disconnection of the brain caused by a focal lesion from structural MR scans. This means that fMRI acquisition in clinical setting is no required. Specifically, LNM operates on the premise that the disconnection between specific brain regions affected by lesions can be evaluated using healthy connectome data. In other words, it involves embedding a specific lesion within a comprehensive normative connectome to determine which brain regions are typically connected to the lesion in a healthy population, thus identifying likely disconnections in patients with that specific lesion (Fox, 2018). LNM has found extensive application in the study of various syndromes arising from brain lesions, including anosognosia, aphasia, and amnesia (Babyar et al., 2019; Boes et al., 2015; Monai et al., 2023). This framework promoted the development of new indirect connectivity measures to study lesion topology or to predict clinical/cognitive outcomes in neurological conditions, such as structural indirect connectivity (Foulon et al., 2018), approaches based on local fiber density (Salvalaggio et al., 2023), those based on graph analysis (Reber et al., 2021), or those based on the structural connectome (Wei et al., 2023). While these new approaches showed promising results in clinical prediction (Salvalaggio et al., 2023; Talozzi et al., 2023; Bowren et al., 2022), we demonstrated that "classical" LNM when applied to predict clinical outcomes in a stroke population shows low predictive power (Pini et al., 2021; Salvalaggio et al., 2021; Salvalaggio et al., 2020). Here, we extended LNM study to GBM, referred to here as functional disconnectivity (FDC). Specifically, we aimed at investigating whether indirect functional disconnection maps computed from a large and well characterized healthy connectome could predict OS in patients with GBM. The results of this study would shed light on the possibility to apply the FDC framework in the neuro-oncology field.

2. Materials and methods

2.1. Lesion data and tumor segmentation

A dataset with $n = 99$ patients with diagnosis of GBM was retrospectively included. Patients were enrolled at the University Hospital (Azienda Ospedale Università di Padova – AOUPD) and the Venetian Institute of Oncology (IOV) of Padova, Italy. The GBM dataset is fully described in Salvalaggio et al. (2023). The whole analytical strategy is reported in Fig. 1. All the procedure was run on Python 3.9 through an ASUS TUF Dash F15 machine (12th Gen Intel(R) Core (TM) i7-12650H 2.30 GHz) running on an Ubuntu 20.04.6 LTS (Focal Fossa) environment. The following libraries were utilized within a conda environment: scikit-learn v1.4.1, scipy v1.9.1, and factor-analyzer v0.4.1.

2.2. Standard protocol approvals, registrations, and patient consents

The study proposal was in accordance with ethical standards of the Declaration of Helsinki and was approved by the Comitato Etico per la Sperimentazione Clinica della Provincia di Padova (No. 70n/AO/20), with no written consent required due the retrospective design.

2.3. Functional disconnections

Lesion masks were non-linearly registered in the MNI space and used as seed ROIs to compute FDC maps (details in (Salvalaggio et al., 2023)). Resting-state functional magnetic resonance (rs-fMRI) data from 173 subjects from the Human Connectome Project (HCP) scanned at 7 Tesla were pre-processed according to the minimal pre-processing pipeline for HCP. Briefly, the data were slice-timing corrected, whole-brain intensity normalized, distortion corrected using synthetic field map estimation, and spatially realigned within and across fMRI runs. Data were regressed to remove sources of spurious variance from head motion (six parameters), the average signal over the whole brain, ventricles, and CSF, and white matter. These masks were identified through Structural MRI segmentation using Freesurfer (https://surfer.nmr.mgh.harvard.edu). Finally, temporal filtering was applied to retain frequencies in the 0.009–0.08-Hz band. Frame censoring was computed using framewise displacement with a threshold of 0.5 mm.

Pre-processed HCP data were then used to compute brain disconnectivity in our sample. To this aim, we applied our enhanced FDC approach that improves the anatomical specificity of functionally disconnected networks through principal component analysis (PC-FDC) (Pini et al., 2021). Specifically, this method involves a first step aimed at identifying a mean (across the connectome) correlation across fMRI volumes between each voxel mapping within the lesion. For each voxel, values were averaged to obtain a single measure expressing the mean connectivity strength between that voxel with the other lesioned voxels. This procedure was repeated for every HCP subject, resulting in a matrix expressing the normative within-connectivity strength between lesioned voxels, which was then fed into a principal component analysis aimed at identifying voxels with the most similar time course within the lesion. According to our previous analysis (Pini et al., 2021), the coefficients of the first PC, explaining the highest amount of variance in the data, were

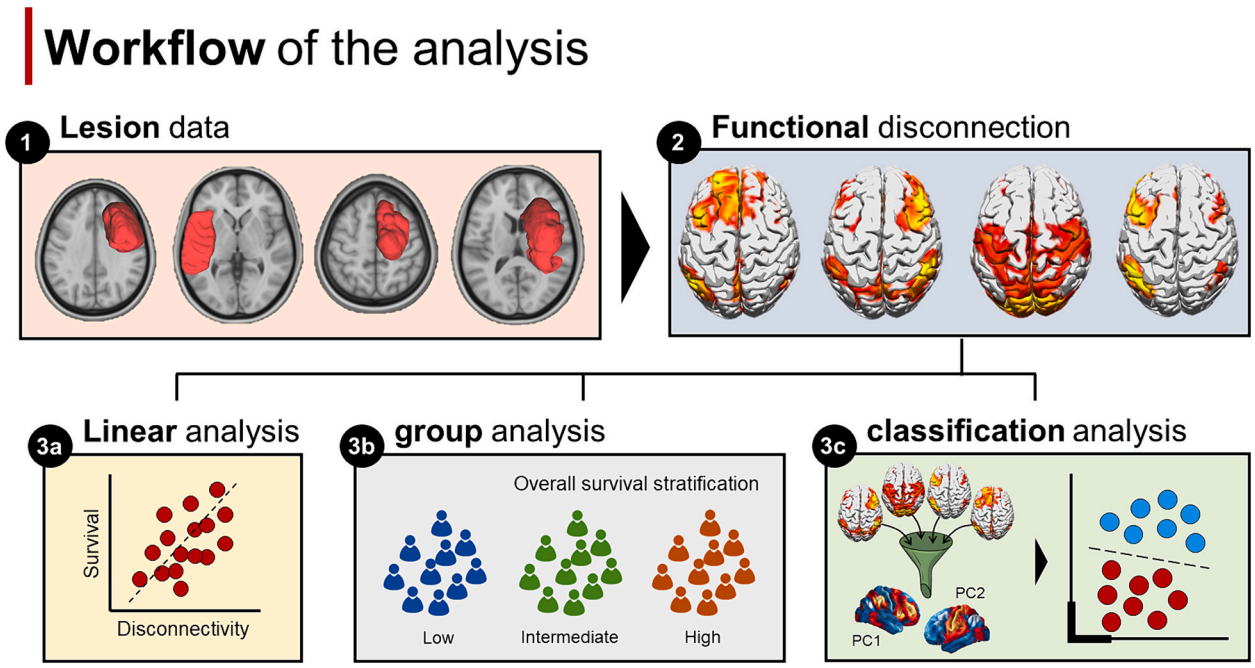

Fig. 1. Workflow of the analysis.
Tumors were segmented (panel 1) and used as masks for computing functional disconnection patterns (panel 2). Different levels of analysis were performed: a linear voxel-wise relationship between overall survival (OS) and network dysconnectivity (panel 3a); a group analysis assessing different network connectivity profiles between patients stratified as low survival (<6 months), intermediate survival (6–20 months) and high OS (>20 months). A classification analysis based on Kmeans and linear discriminant algorithms to predict patients with different degrees of OS.

projected back to the lesion space and only voxels with absolute coefficients higher than the 20th percentile of the distribution were considered. Finally, these PC1 lesion-voxels were used as seed ROIs to compute whole brain seed-connectivity voxel-wise analysis, according to standard procedure (Boes et al., 2015). For the present analysis, PC-FDC maps were computed using the tumor core masks (including both areas of contrast and non-contrast enhancement and necrotic tissue), without considering the edema. The PC-FDC approach separates gray and white matter involvement of lesions by computing different maps for each tissue (Pini et al., 2021).

2.4. Network description

For each disconnectivity map we computed the spatial correlation with Yeo's 7 networks atlas. Analysis of variance (ANOVA) was run to compare disconnectivity pattern across networks. Before running the ANOVA, we checked for the homoscedasticity of the data using the Levene's test. For data with unequal variance, we used the Welch ANOVA which better controls for type I error in case of heterogeneity of variance (Liu, 2015).

2.5. Overall survival regression and classification

First, a linear regression approach was applied to investigate the association between OS and network disconnectivity. A nonparametric inference based on FSL-randomise with $n = 1000$ permutations was applied. Multiple comparisons were corrected across space using a family-wise error (FWE) based on permutation testing at a threshold-free cluster enhancement (TFCE). Significance was set at a p-value <0.05. To account for the influence of age and core size, we included these factors as covariates in the voxel-wise analysis. The analysis was conducted using a conservative approach, wherein PC-FDC maps were thresholded with an arbitrary cut-off of 0.2. Additionally, a sensitivity analysis was performed employing a more liberal approach, without applying any threshold to the maps.

Second, patients were stratified into three different groups based on overall survival. A first group highlighted patients with low survival, defined as OS <6 months. An intermediate group consisted of patients with a survival range between 6 and 20 months. A third group was characterized by patients with an overall survival above 20 months. Compared to Fyllingen's study we set a high survival threshold to 20 months for creating groups with comparable size (Fyllingen et al., 2021). These groups roughly correspond to the 33° and 66° percentile of OS distribution values. Network disconnectivity between groups was compared through a non-parametric procedure (TFCE with $n = 1000$, significant level set to pFWE<0.05). Age and lesion size were included as covariates. Further, from the network maps the average connectivity network strength was computed for each participant. ANOVA was run to compare network strength across groups, as described above (*2.3 Network description)*. Both group voxel-wise analysis and average network strength were computed using a liberal (unthreshold) and a conservative (threshold >0.2) approach.

Moreover, for each participant, network maps were associated to a specific Yeo's map through a "winner-take-all-approach" based on spatial correlation (Pearson's coefficient). A chi square statistic was applied to investigate whether OS groups showed a different distribution on network assignments. Additionally, we carried out an additional analysis to assess the differences in correlation between network maps and network templates between groups using a repeated measures ANOVA. This analysis included the network template as the within factor and group as the between factor. The interaction between group and network was significant at $p < 0.05$.

Finally, we checked the classification accuracy of network disconnectivity patterns in predicting patients belonging to the low, intermediate, or high survival group (Fyllingen et al., 2021). To this end, a principal component analysis (PCA) was applied to the thresholded (conservative) network maps (in voxel space). Kaiser-Meyer-Olkin (KMO) test was run to test the sampling adequacy of the PCA. The PCs explaining >90% of the variance were used as features in a Kmeans algorithm. Each time we executed the Kmeans algorithm, we evaluated

two groups to examine the alignment between OS groups ($n = 2$) and connectivity-based clusters (fixed at k = 2). The OS groups were subsequently compared in pairs to evaluate the consistency between survival stratification and connectivity-based clusters. Classification accuracy was then computed. The same analysis was performed considering the (liberal) unthresholded maps. To ensure the prediction was not influenced by the algorithm selection, we also run a linear discriminant analysis (LDA) with leave-one-out hyperparameter validation (solver: singular value decomposition; least squares; eigenvalue decomposition) splitting the dataset into train (using the 60% of the total dataset) and test sets. The same approach, comparing each time two groups with two connectivity-classes, was adopted considering the original classification of the three OS groups (Fyllingen et al., 2021).

Additionally, the Kmeans analysis was repeated considering the extreme groups (lowest vs highest survivors) using different OS percentile for the stratification: i) 50th percentile; ii) 25th and 75th percentiles; and 20th and 80th percentiles.

Finally, we conducted an analysis to investigate whether a similar network topology among patients could be utilized for predicting OS. Our approach involved partitioning the GBM dataset into two equal-sized groups, each comprising 49 patients, with one patient randomly excluded to avoid unbalanced datasets. We employed the Kuhn–Munkres algorithm (Kuhn, 1955) and used 'earson's correlation as the distance metric between thresholded PC-FDC maps to pair up the patients. The OS of one patient in each pair was used to predict the OS of the other patient, and we calculated the corresponding R value across the entire sample. This process was repeated iteratively for a total of $n = 1000$ random dataset splits. A high mean distribution of R values would indicate a potential relationship between PC-FDC network topology and OS. Further, the mean absolute error (MAE) between predicted and real OS was compared with a random distribution built using n = 1000 permutations.

2.6. Connectivity projection into a 2D space

Finally, we explored the relationship between indirect functional connectivity and OS projecting the thresholded PC-FDC maps into a 2D space by means of the Uniform Manifold Approximation and Projection (UMAP) algorithm, a non-linear embedding approach that distributes data variability along major axes (McInnes et al., 2018). We employed UMAP for its ability to transform data onto a low dimensional space maintaining the original structure of the data. Thus, patients with similar disconnectivity profile cluster together in the 2D space, while patients with different distribution of connectivity are located further apart. The visualization was complemented by highlighting patients within the various OS class distributions (low, intermediate, and high). UMAP was executed for both volumetric maps, which included only the gray matter masks using the Harvard-Oxford gray matter maps with a 50% probability, and surface maps (MNI maps projected onto the fsaverage 164 K vertices space) for the left and right hemispheres separately. Variance explained by the 2D dimensions of UMAP was computed considering UMAP as an approximation of the original matrix X (m × n connectivity data, where m = number of voxels/vertices and n = number of patients) and fitting a partial least square model

$$X = \alpha + \beta\ UMAP\ matrix + \varepsilon$$

and estimate the fraction of data variance explained by UMAP components via R-squared.

Finally, a Gaussian mixture model (GMM) with three classes was employed on the UMAP (defined by GM-masked volume) to evaluate the alignment between the 2D network space and the overall survival (OS) categorization.

3. Results

Mean age of the patients included was 62 ± 12, with 29% being female and an overall mean survival rate of 14 ± 10. The frequency map of the core GBM distribution is reported in Fig. 2.

3.1. Network disconnectivity involvement

Results are shown in Fig. 2**.** We reported a significant difference in terms of similarity between disconnectivity maps ($p < 0.001$). Specifically, disconnectivity maps showed the highest spatial similarity with the sensory (sensory-motor, and visual) and attentional networks (ventral and dorsal attentional networks), while the frontoparietal and memory networks (default mode and limbic networks) showed the lowest similarity pattern.

3.2. Linear relationships with overall survival

No negative and positive relations were reported between network disconnection strength and overall survival in the whole cohort of patients surviving at the multiple comparison threshold ($p > 0.05$ FWE). When we applied a less stringent threshold ($p < 0.001$ uncorrected) we confirmed no-significant effects surviving the threshold. These results were reported for both the (liberal) unthresholded and (conservative) thresholded maps, with or without the inclusion of age and lesion size as covariates.

3.3. Survival group analysis

When patients were compared based on OS stratification, we found no significant differences in network connectivity at voxel-wise level (for both the liberal and conservative thresholding approaches), regardless of the inclusion of age and lesion size as covariates. Null results were observed for the full contrasts matrix (low vs high; low vs intermediate, and high vs intermediate). Null results were observed with a threshold corrected for multiple comparison (pFWE<0.05). Similar null results were reported applying a less stringent threshold ($p < 0.001$ uncorrected). Similarly, the ANOVA comparing network disconnectivity strength showed comparable patterns across groups (unthresholding: $p = 0.201$; unthreshlding: $p = 0.909$). Mean maps from the three groups showed high spatial similarity ($r > 0.9$ for all the groups). Finally, the Chi square statistics applied on network distribution (winner-take-all approach) suggested that similar disconnectivity patterns were observed across OS groups. These results were confirmed when we assessed differences between groups using correlation network-template measures. A significant network effect was observed ($p < 0.001$), while group ($p = 0.223$), and group*network interaction term ($p = 0.909$) were not significant, suggesting a similar connectivity patterns across survival groups. Results are shown in **Fig.** 3 (conservative threshold) and Fig. 4 (liberal threshold).

3.4. Classification accuracy based on network patterns

A principal component analysis on the whole cohort revealed that the first 5 components explained >90% of the variance, in line with previous studies in stroke patients (Salvalaggio et al., 2020). Thus, we retained these components to investigate classification accuracy of network patterns into OS groups ($n_{low} = 27$, $n_{intermediate} = 44$, $n_{high} = 28$). Results showed a low accuracy classification score (around 50%) for the full set of comparisons (see Fig. 3). Similar results were reported for the LDA (low vs high: accuracy test set: 52%; high vs intermediate: accuracy test set: 50%; low vs intermediate: accuracy test set: 52%). When we applied the same analysis to the unthresholded maps, we obtained comparable classification accuracy results, approximately 50%, using the K-means algorithm (Fig. 4).

A low classification accuracy was reported when patients were stratified into low and high survivors using different distribution of OS values (50th percentile: accuracy = 53% $n_{low} = 49$, $n_{high} = 50$; 25th vs 75th percentile: accuracy = 54%, $n_{low} = 25$, $n_{high} = 25$; 20th vs 80th

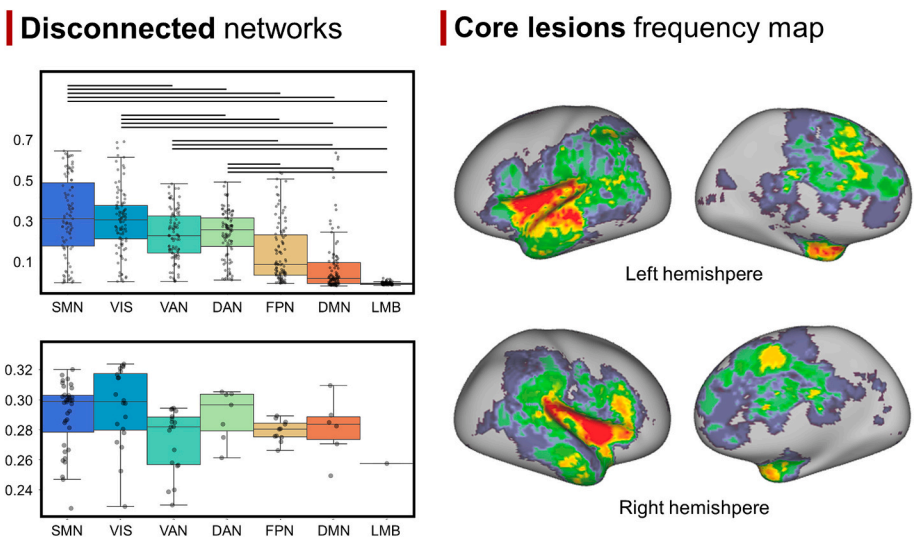

Fig. 2. Network disconnectivity.
Top left panel: disconnectivity patterns in glioblastoma showed the highest similarity with sensory and attentional networks. Black lines represent post-hoc significant comparison between networks. Bottom left panel: each PC-FDC is assigned to a specific network template through a 'winner-take-all-approach' based on spatial correlation values; no significant differences were reported in terms of network disconnectivity strength between networks in the whole cohort. Right panel: Frequency map of core glioblastoma masks included in the analysis.

percentile: accuracy = 53%, n_{low} = 20, n_{high} = 20) compared with kmeans connectivity-clusters based on the thresholded connectivity maps.

Finally, patient matching based on PC-FDC similarity did not yield consistent OS outcomes. Although the MAE between real and predicted OS compared with a random distribution showed significant lower values ($t = 2.93$; $p = 0.003$), the average correlation between observed OS and the OS predicted for patients sharing a similar PC-FDC profile was near to zero ($r_{mean} = 0.02$). The highest and lowest correlation values within the distribution ($n = 1000$) hovered around 0.45 and −0.35, respectively (Fig. 3). These results underscore a notably limited alignment between PC-FDC similarity and OS across patients.

3.5. UMAP space

As reported in Fig. 5, connectivity maps projected onto a 2D space did not exhibit a clear association with OS classification, thereby confirming the linear results described previously. The 2D UMAP dimensions explained 30%, 31%, and 38% of the variance of the PC-FDC maps for volume, left surface, and right surface, respectively. The absence of a distinct connection between OS and indirect connectivity outcomes was observed in both volumetric and surface-projected PC-FDC maps. The GMM applied to the 2D UMAP volume maps reveals a distinctly separated space. For each GMM class, a mean cortical map was computed by averaging across all the maps falling into that class. The results indicate a separation within the dorsal-attention, ventral-attention, and sensorimotor networks, consistent with the findings of the network disconnectivity analysis (section 3.1). The lack of correspondence between the GMM and overall survival (OS) classes confirms the absence of a relationship between indirect connectivity and clinical outcomes.

4. Discussion

We performed a comprehensive investigation to determine whether FDC could serve as predictors for OS in patients diagnosed with GBM. We reported that GBM maps onto sensorial and attentional networks, in line with the load of the core lesion over these networks (Sansone et al., 2023). DAN results are in line with a previous study by Mandal et al. reporting evident tumor-DAN connectivity across a large cohort of patients with gliomas related to long-term postsurgical outcomes attentional functions (Mandal et al., 2024). While Mandal's study assessed connectivity through participant's functional scan, our indirect analyses consistently revealed a lack of any significant relationship between OS and indirect functional connectivity outcomes. This null association persisted when we assessed the relationship with OS at a voxel-wise level. Additionally, our attempts to predict OS, both as a categorical and continuous variable, using PC-FDC maps, were unsuccessful. The volume and topology of the GBM lesions did not predict the clinical outcome of GBM (Salvalaggio et al., 2023).

Indirect functional metrics have been widely employed to explore whether different neurological syndromes are linked to specific network disruptions following brain lesions (Fox, 2018; Boes et al., 2015; Monai et al., 2023). However, when applied to predict cognitive deficits in a clinical stroke population, the predictive value of FDC was found to be lower compared to using lesion-based metrics (Pini et al., 2021; Salvalaggio et al., 2020). These findings strongly imply that cognitive and clinical outcomes are influenced by numerous factors, including neural effects involving both structural and functional reorganization in regions distant from the initial lesion (Griffis et al., 2019). Indirect approaches are limited in their ability to describe these secondary and distal changes, only capturing the primary level of disconnection. Consequently, they fall short of providing significant insights into the prediction of behavioral deficits following brain lesions. We expanded upon and reinforced this perspective within our study of patients with GBM. This complexity is further compounded by the fact that the solid component of gliomas exhibits substantial functional connectivity with remote brain regions. Sprugnoli and colleagues (2022) observed a significant association between this connectivity pattern and individual OS (Sprugnoli et al., 2022), suggesting widespread alterations which can explain different OS between patients.

Recently, we have shown that indirect approaches based on structural data can lead to more accurate OS predictions (Salvalaggio et al., 2023). Specifically, in our prior work we did not focus on the disconnection caused by GBM but instead examined a local property, the number of fibers affected by GBM, inferred from a normative dataset. Employing a normative structural connectome atlas, we calculated the average number of fibers encompassing each brain tumor, effectively condensing each tumor into a single value termed the track density index (TDI). This approach differs from FDC, as it is based on the

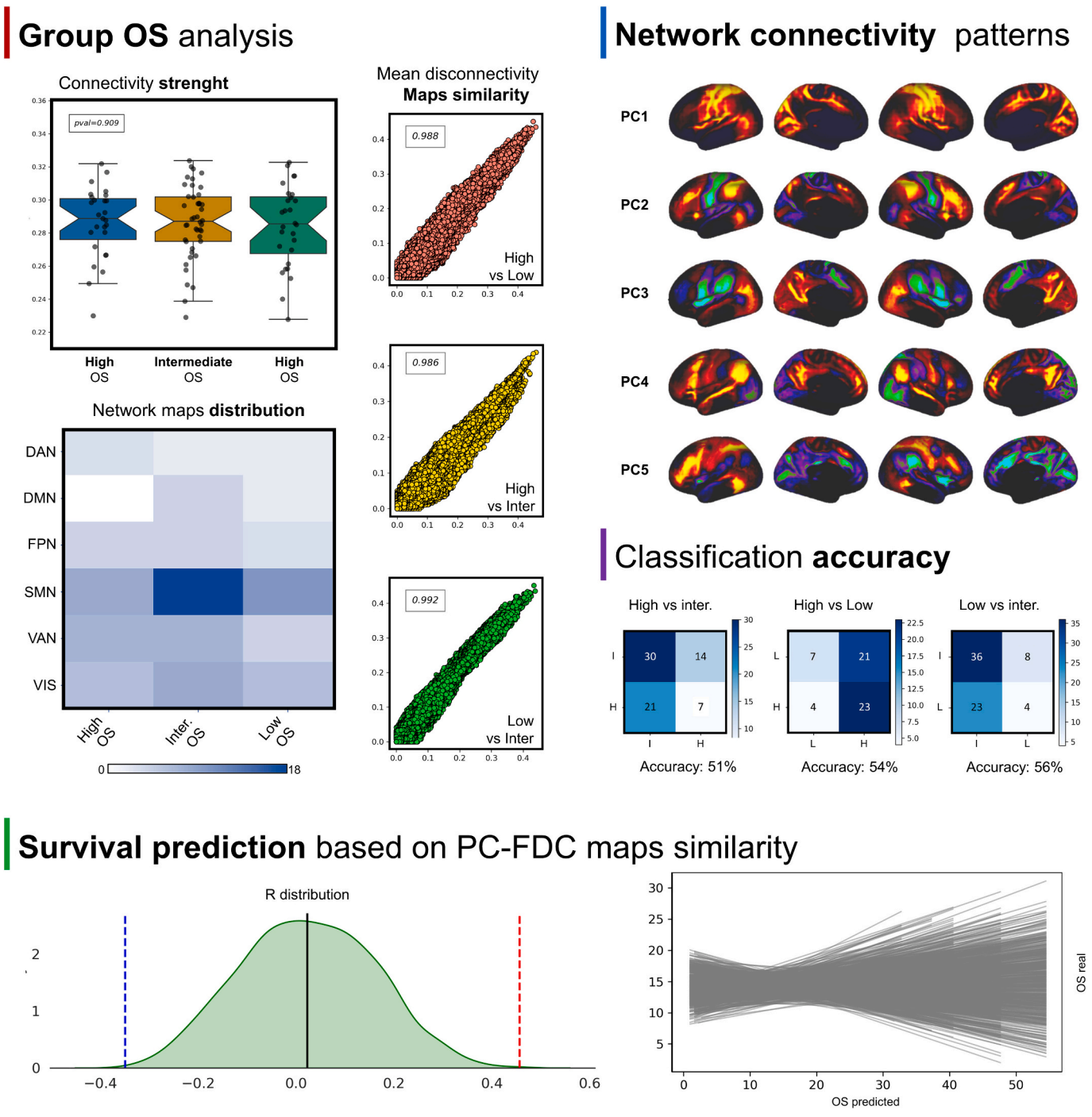

Fig. 3. OS groups and network disconnectivity.
Top left panels: network strength outcome (left-top-panel) and network distribution (left-bottom panel) was similar across OS groups. Group-average maps within the three survival groups showed similar spatial patterns. Top right panels: five components, explaining >90% of the disconnectivity variance (top panel), were entered in a Kmeans algorithm to classify survival groups showing very low classification accuracy. Bottom panels: patients were matched in a 1:1 fashion based on PC-FDC maps spatial correlation. The overall survival (OS) of a patient was used as predictive OS of the corresponding assigned patient and the R-value was computed between the 'predicted' and the observed OS. The procedure was iteratively repeated ($n = 1000$). Low R values were reported suggesting a null relationship between PC-FDC maps similarity and OS.

computation of indirect functional connectivity maps. We showed a significant association between TDI and OS, surpassing relationships with classical prognostic factors such as age, genetics, and health status[23]. The underlying assumption in our approach is different in nature: we hypothesized that regions with higher fiber density would result in a poorer prognosis due to higher potential for cancer cells to spread within the brain. Our previous results align with prior research that demonstrated how GBM can lead to widespread disruptions in structural connectivity beyond the focal lesion, which play a crucial role in mediating patient survival (Wei et al., 2023). In contrast, the current findings underscore that greater indirect functional disconnection does not necessarily correlate with a worse prognosis for these patients. Although on the surface, these results might appear contradictory – where structural disconnections are predictive of OS compared to

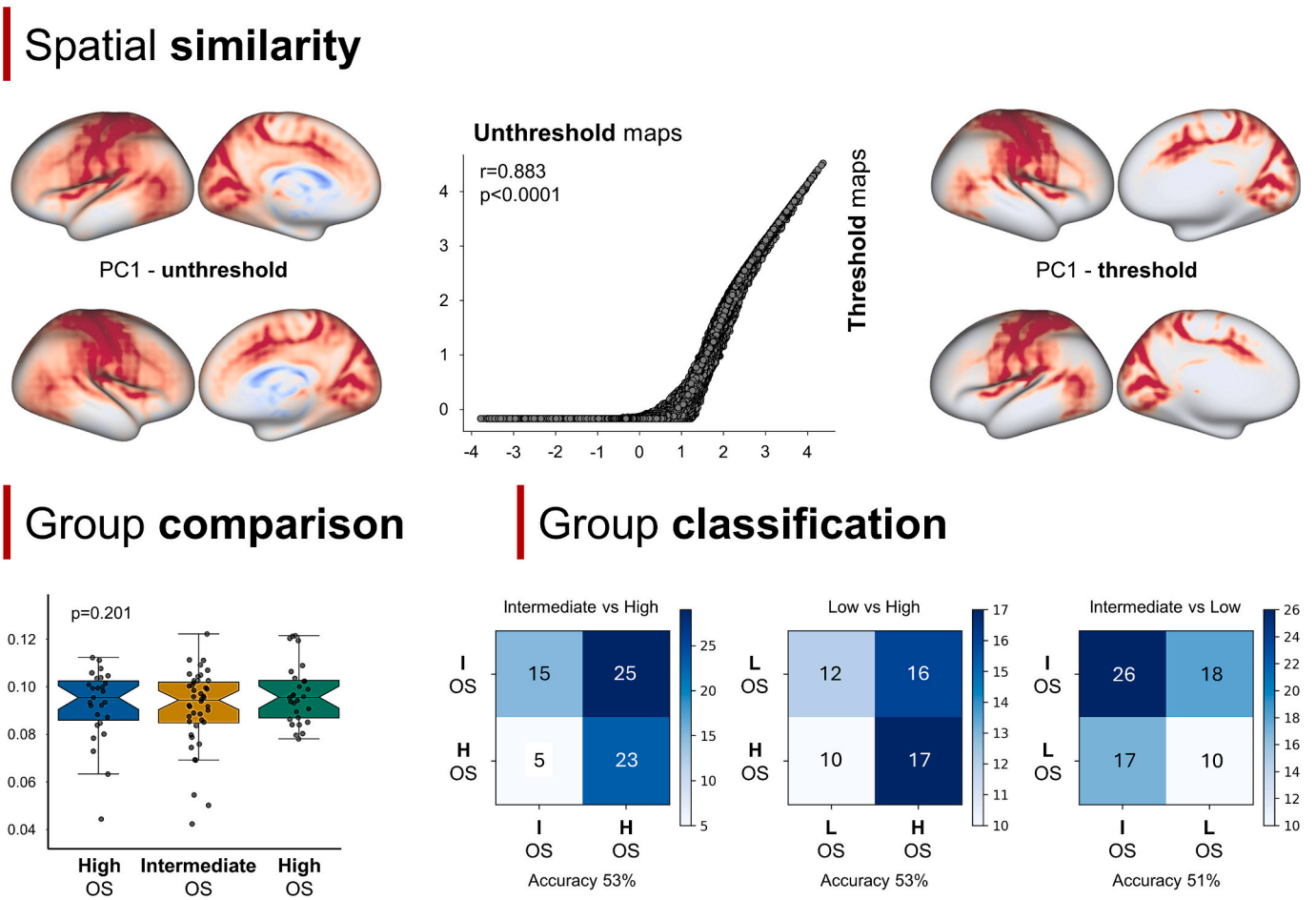

Fig. 4. Top panels display the comparison between the whole group PC1 for the unthresholded (left) and thresholded (right) connectivity maps. A high spatial overlap ($r > 0.88$) is observed between these two patterns. In the bottom panel, statistical analysis compares network strength between survival groups (left) and the classification procedures (right) for the unthresholded maps. Consistently, similar null relationships between network connectivity/patterns and overall survival are observed, echoing the results from thresholded maps.

functional disconnection – they are consistent with our previous study. In our earlier work, we observed a similar pattern in the context of patients with stroke. Specifically, while structural disconnections could effectively predict cognitive deficits in patients with stroke in a manner similar to lesion-based outcomes, the application of the same predictive model to indirect functional disconnection in patients with stroke yielded very low predictive accuracy (Salvalaggio et al., 2020). These consistent findings suggest that the relationship between structural and functional connectivity and their predictive value for patient outcomes can underlie different processes. That is, while structural disconnections computed from a healthy connectome might represent a more reliable and homogeneous proxy of the alterations occurring in patients, functional alterations might undergo more complex patterns, such as network unbalance, plasticity mechanisms and arising of both hyper- and/or hypo-synchrony patterns. The latter has been consistently reported following brain stroke lesions (Corbetta et al., 2018), traumatic brain injury (Mayer et al., 2011), neurodegenerative disorders (Hillary and Grafman, 2017) and preliminary reports suggest a similar phenotype in brain gliomas (Ng et al., 2022; Zhang et al., 2018). Further, high functional variability is reported among adults, influencing cognitive performance (Boylan et al., 2021). Moreover, a possibility linked to the low relationship could be attributed to the properties of GBM. In contrast to stroke lesions, GBM may displace surrounding tissues rather than causing complete disconnection. This effect cannot be captured by FDC, as this approach assumes a complete disconnection of the lesion mask from the rest of the brain. Further studies should investigate whether this effect primarily influences the low prediction reported in this study.

Some limitations of our study should be considered when interpreting the findings. First, PC-FDC maps were built using GBM core regions, potentially overlooking the influence of surrounding edema. Edema, a common feature of GBM, may introduce additional complexities in the functional connectivity patterns that were not fully accounted for in our analysis. Similarly, further studies should aim to assess whether functional maps constructed using various definitions of core tumor (e.g., contrast-enhanced versus non-contrast enhancement or necrotic tissue) could yield divergent results. Second, our study did not directly address the prediction of cognitive deficits. Further investigations specifically designed to assess the predictive value of FDC for cognitive deficits in patients with GBM are warranted to offer a more comprehensive perspective on the clinical implications of our findings. Finally, while 7 T offers higher spatial resolution and enhanced sensitivity compared to FDC generated with lower field strengths such as 3 T (see Fig. 1 from (Salvalaggio et al., 2021)), it might pose challenges related to signal-to-noise ratio, which deserve future investigations in this emerging cancer neuroscience field.

5. Conclusions

In summary, our study explored the potential of FDC as prognostic indicators for OS in GBM. Our comprehensive analysis consistently revealed no significant relationship between OS and these measures.

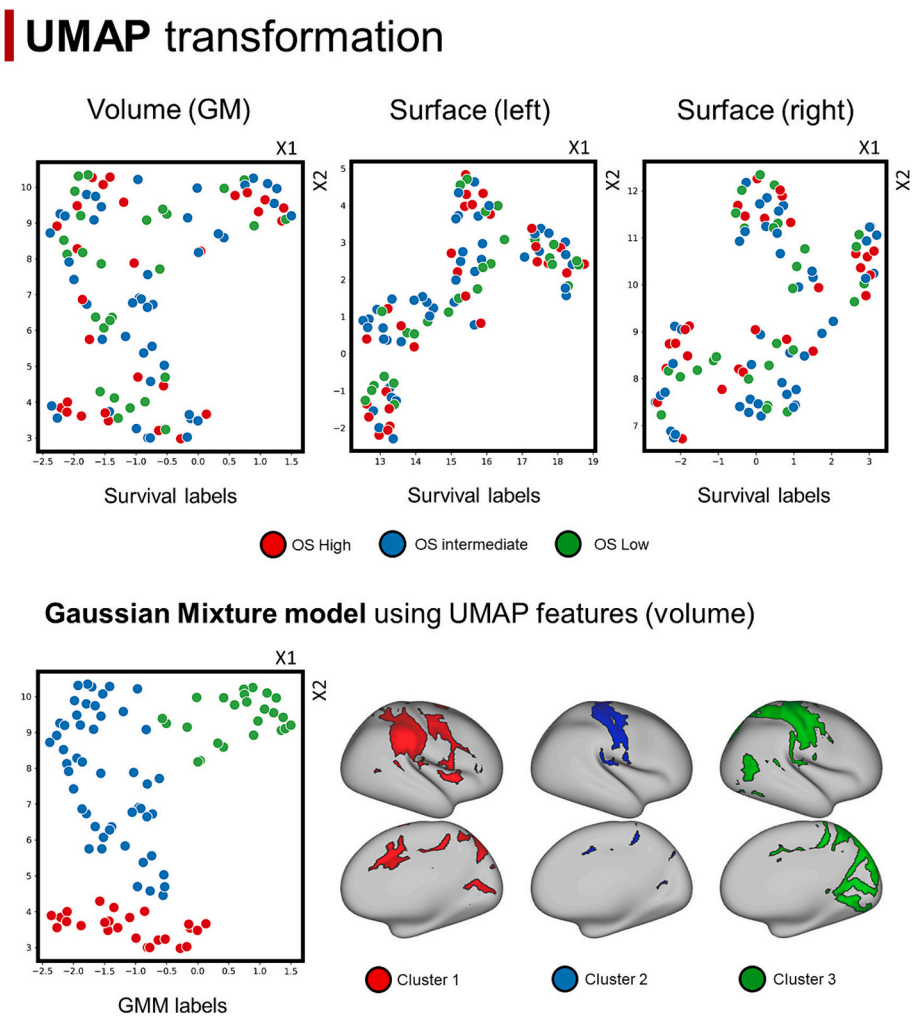

Fig. 5. Spatial connectivity maps projected into a 2D space.
Top panels: each plot represents an individual patient ($n = 99$) projected into a two-dimensional space using the indirect connectivity outcomes. No clear association between overall survival (OS) and indirect connectivity maps was observed. The absence of a clear association was reported for maps in the volume space (left panel) as well as those projected onto the left (central panel) and right surface (right panel). Bottom Panel: UMAP features (derived from volume) were clustered into three groups using the Gaussian mixture model. These groups were organized within a distinct space defined by networks encompassing the ventral attention (red), motor network (blue), and dorsal attention (green). The segregation into these three network clusters did not align with the overall survival categorization. (For interpretation of the references to colour in this figure legend, the reader is referred to the web version of this article.)

Our findings, align with a broader perspective we observed in stroke patients. The consistent lack of a substantial relationship between FDC and patient outcomes, raises questions about its practical utility as a reliable clinical tool for predicting overall survival in patients with GBM. This highlights the importance of considering alternative methods and more robust predictive models when addressing clinical decisions and treatment strategies in the context of GBM.

Funding

MC was supported by Fondazione Cassa di Risparmio di Padova e Rovigo (CARIPARO) - Ricerca Scientifica di Eccellenza 2018 (Grant Agreement number 55403); Italian Ministero della Salute, Brain connectivity measured with high-density electroencephalography: a novel neurodiagnostic tool for stroke (NEUROCONN; RF-2018-1236689); Horizon 2020 European School of Network Neuroscience - European School of Network Neuroscience (euSNN), H2020-SC5-2019-2 (Grant Agreement number 860563); Horizon 2020 research and innovation program; Visionary Nature Based Actions For Heath, Wellbeing & Resilience in Cities (VARCITIES), Horizon 2020-SC5-2019-2 (Grant Agreement number 869505); Italian Ministero della Salute: Eye-movement dynamics during free viewing as biomarker for assessment of visuospatial functions and for closed-loop rehabilitation in stroke (EYEMOVINSTROKE; RF-2019-12369300), HORIZON-ERC-SyG (Grant No.101071900).

Author contributions

LP contributed to the conceptualization, design, methodology, imaging and statistical analysis, interpretation, data visualization, and writing of the draft; GL, GS, MG, MP, FV, and LD contributed to data acquisition and revising the draft; MC and AS contributed to data interpretation, supervision and revising the draft.

Founding

MC was supported by Fondazione Cassa di Risparmio di Padova e Rovigo (CARIPARO) – Ricerca Scientifica di Eccellenza 2018 (Grant Agreement number 55403); Italian Ministero della Salute, Brain connectivity measured with high-density electroencephalography: a novel neurodiagnostic tool for stroke (NEUROCONN; RF-2018-1236689); Horizon 2020 European School of Network Neuroscience – European

School of Network Neuroscience (euSNN), H2020-SC5-2019-2 (Grant Agreement number 860563); Horizon 2020 research and innovation program; Visionary Nature Based Actions For Heath, Wellbeing & Resilience in Cities (VARCITIES), Horizon 2020-SC5-2019-2 (Grant Agreement number 869505); Italian Ministero della Salute: Eye-movement dynamics during free viewing as biomarker for assessment of visuospatial functions and for closed-loop rehabilitation in stroke (EYEMOVINSTROKE; RF-2019-12369300), HORIZON-ERC-SyG (Grant No.101071900); HORIZON- INFRA-2022 SERV (Grant No. 101147319) "EBRAINS 2.0: A Research Infrastructure to Advance Neuroscience and Brain Health".

CRediT authorship contribution statement

Lorenzo Pini: Writing – review & editing, Visualization, Validation, Software, Methodology, Investigation, Formal analysis, Data curation, Conceptualization. **Giuseppe Lombardi:** Writing – review & editing, Resources. **Giulio Sansone:** Writing – review & editing. **Matteo Gaiola:** Writing – review & editing. **Marta Padovan:** Writing – review & editing. **Francesco Volpin:** Writing – review & editing. **Luca Denaro:** Writing – review & editing. **Maurizio Corbetta:** Writing – review & editing, Validation, Supervision. **Alessandro Salvalaggio:** Writing – review & editing, Validation, Supervision.

Declaration of competing interest

Drs Salvalaggio and Pini and Prof Corbetta reported a patent pending (102022000015360). No other disclosures are reported.

Data availability

Data will be made available on request.

References

Babyar, S.R., Smeragliuolo, A., Albazron, F.M., Putrino, D., Reding, M., Boes, A.D., 2019. Lesion localization of poststroke lateropulsion. Stroke 50 (5), 1067–1073. https://doi.org/10.1161/STROKEAHA.118.023445.

Boes, A.D., Prasad, S., Liu, H., et al., 2015. Network localization of neurological symptoms from focal brain lesions. Brain 138 (10), 3061–3075. https://doi.org/10.1093/brain/awv228.

Bowren, M., Bruss, J., Manzel, K., et al., 2022. Post-stroke outcomes predicted from multivariate lesion-behaviour and lesion network mapping. Brain 145 (4), 1338–1353. https://doi.org/10.1093/brain/awac010.

Boylan, M.A., Foster, C.M., Pongpipat, E.E., Webb, C.E., Rodrigue, K.M., Kennedy, K.M., 2021. Greater BOLD variability is associated with poorer cognitive function in an adult lifespan sample. Cereb. Cortex 31 (1), 562–574. https://doi.org/10.1093/cercor/bhaa243.

Buckner, R.L., Snyder, A.Z., Shannon, B.J., et al., 2005. Molecular, structural, and functional characterization of Alzheimer's disease: evidence for a relationship between default activity, amyloid, and memory. J. Neurosci. 25 (34), 7709–7717. https://doi.org/10.1523/JNEUROSCI.2177-05.2005.

Corbetta, M., Siegel, J.S., Shulman, G.L., 2018. On the low dimensionality of behavioral deficits and alterations of brain network connectivity after focal injury. Cortex 107, 229–237. https://doi.org/10.1016/j.cortex.2017.12.017.

Daniel, A.G.S., Park, K.Y., Roland, J.L., et al., 2021. Functional connectivity within glioblastoma impacts overall survival. Neuro-Oncology. 23 (3), 412–421. https://doi.org/10.1093/neuonc/noaa189.

Foulon, C., Cerliani, L., Kinkingnéhun, S., et al., 2018. Advanced lesion symptom mapping analyses and implementation as BCBtoolkit. GigaScience 7 (3). https://doi.org/10.1093/gigascience/giy004.

Fox, M.D., 2018. Mapping symptoms to brain networks with the human connectome. N. Engl. J. Med. 379 (23), 2237–2245. https://doi.org/10.1056/NEJMra1706158.

Fyllingen, E.H., Bø, L.E., Reinertsen, I., et al., 2021. Survival of glioblastoma in relation to tumor location: a statistical tumor atlas of a population-based cohort. Acta Neurochir. 163 (7), 1895–1905. https://doi.org/10.1007/s00701-021-04802-6.

Gilbert, M.R., Wang, M., Aldape, K.D., et al., 2013. Dose-dense temozolomide for newly diagnosed glioblastoma: a randomized phase III clinical trial. JCO 31 (32), 4085–4091. https://doi.org/10.1200/JCO.2013.49.6968.

Griffis, J.C., Metcalf, N.V., Corbetta, M., Shulman, G.L., 2019. Structural disconnections explain brain network dysfunction after stroke. Cell Rep. 28 (10), 2527–2540.e9. https://doi.org/10.1016/j.celrep.2019.07.100.

Hillary, F.G., Grafman, J.H., 2017. Injured brains and adaptive networks: the benefits and costs of Hyperconnectivity. Trends Cogn. Sci. 21 (5), 385–401. https://doi.org/10.1016/j.tics.2017.03.003.

Illic, R., Somma, T., Savic, D., et al., 2017. A survival analysis with identification of prognostic factors in a series of 110 patients with newly diagnosed glioblastoma before and after introduction of the Stupp regimen: a single-center observational study. World Neurosurg. 104, 581–588. https://doi.org/10.1016/j.wneu.2017.05.018.

Kuhn, H.W., 1955. The Hungarian method for the assignment problem. Nav. Res. Logist. 2 (1–2), 83–97. https://doi.org/10.1002/nav.3800020109.

Lin, D., Wang, M., Chen, Y., et al., 2021. Trends in intracranial glioma incidence and mortality in the United States, 1975-2018. Front. Oncol. 11, 748061 https://doi.org/10.3389/fonc.2021.748061.

Liu, Hangcheng. Comparing Welch ANOVA, a Kruskal-Wallis test, and traditional ANOVA in case of heterogeneity of variance. Virginia Commonwealth University, 2015.

Mandal, A.S., Brem, S., Suckling, J., 2023. Brain network mapping and glioma pathophysiology. Brain Commun. 5 (2), fcad040 https://doi.org/10.1093/braincomms/fcad040.

Mandal, A.S., Wiener, C., Assem, M., et al., 2024. Tumour-infiltrated cortex participates in large-scale cognitive circuits. Cortex 173, 1–15. https://doi.org/10.1016/j.cortex.2024.01.004.

Mansouri, A., Brar, K., Cusimano, M.D., 2020. Considerations for a surgical RCT for diffuse low-grade glioma: a survey. Neuro-Oncol. Pract. 7 (3), 338–343. https://doi.org/10.1093/nop/npz058.

Mayer, A.R., Mannell, M.V., Ling, J., Gasparovic, C., Yeo, R.A., 2011. Functional connectivity in mild traumatic brain injury. Hum. Brain Mapp. 32 (11), 1825–1835. https://doi.org/10.1002/hbm.21151.

McInnes, L., Healy, J., Saul, N., Großberger, L., 2018. UMAP: Uniform manifold approximation and projection. JOSS 3 (29), 861. https://doi.org/10.21105/joss.00861.

Monai, E., Pini, L., Palacino, F., et al., 2023. Convergence of Visual and Motor Awareness in Human Parietal Cortex. Ann. Neurol. https://doi.org/10.1002/ana.26791. Published online October 11. ana.26791.

Ng, S., Deverdun, J., Lemaitre, A.L., et al., 2022. Precuneal gliomas promote behaviorally relevant remodeling of the functional connectome. J. Neurosurg. 1–11. https://doi.org/10.3171/2022.9.JNS221723. Published online October 1.

Osswald, M., Jung, E., Sahm, F., et al., 2015. Brain tumour cells interconnect to a functional and resistant network. Nature 528 (7580), 93–98. https://doi.org/10.1038/nature16071.

Ostrom, Q.T., Gittleman, H., Stetson, L., Virk, S., Barnholtz-Sloan, J.S., 2018. Epidemiology of intracranial gliomas. In: Chernov, M.F., Muragaki, Y., Kesari, S., IE, McCutcheon (Eds.), Progress in Neurological Surgery, Vol 30, pp. 1–11. https://doi.org/10.1159/000464374. S. Karger AG.

Palmqvist, S., Schöll, M., Strandberg, O., et al., 2017. Earliest accumulation of β-amyloid occurs within the default-mode network and concurrently affects brain connectivity. Nat. Commun. 8 (1), 1214. https://doi.org/10.1038/s41467-017-01150-x.

Pandit, R., Chen, L., Götz, J., 2020. The blood-brain barrier: physiology and strategies for drug delivery. Adv. Drug Deliv. Rev. 165-166, 1–14. https://doi.org/10.1016/j.addr.2019.11.009.

Pereira, J.B., Ossenkoppele, R., Palmqvist, S., et al., 2019. Amyloid and tau accumulate across distinct spatial networks and are differentially associated with brain connectivity. eLife 8, e50830. https://doi.org/10.7554/eLife.50830.

Pini, L., Jacquemot, C., Cagnin, A., et al., 2020. Aberrant brain network connectivity in presymptomatic and manifest Huntington's disease: a systematic review. Hum. Brain Mapp. 41 (1), 256–269. https://doi.org/10.1002/hbm.24790.

Pini, L., Salvalaggio, A., De Filippo De Grazia, M., Zorzi, M., Thiebaut de Schotten, M., Corbetta, M., 2021. A novel stroke lesion network mapping approach: improved accuracy yet still low deficit prediction. Brain Commun. fcab259. https://doi.org/10.1093/braincomms/fcab259. Published online November 13.

Reber, J., Hwang, K., Bowren, M., et al., 2021. Cognitive impairment after focal brain lesions is better predicted by damage to structural than functional network hubs. Proc. Natl. Acad. Sci. USA 118 (19), e2018784118. https://doi.org/10.1073/pnas.2018784118.

Salvalaggio, A., De Filippo De Grazia, M., Zorzi, M., Thiebaut de Schotten, M., Corbetta, M., 2020. Post-stroke deficit prediction from lesion and indirect structural and functional disconnection. Brain 143 (7), 2173–2188. https://doi.org/10.1093/brain/awaa156.

Salvalaggio, A., De Filippo De Grazia, M., Pini, L., Thiebaut De Schotten, M., Zorzi, M., Corbetta, M., 2021. Reply: Lesion network mapping predicts post-stroke behavioural deficits and improves localization. Brain 144 (4), e36. https://doi.org/10.1093/brain/awab004.

Salvalaggio, A., Pini, L., Gaiola, M., et al., 2023. White matter tract density index prediction model of overall survival in glioblastoma. JAMA Neurol. https://doi.org/10.1001/jamaneurol.2023.3284. Published online September 25.

Sansone, G., Pini, L., Salvalaggio, A., et al., 2023. Patterns of gray and white matter functional networks involvement in glioblastoma patients: indirect mapping from clinical MRI scans. Front. Neurol. 14, 1175576. https://doi.org/10.3389/fneur.2023.1175576.

Sporns, O., 2013. Structure and function of complex brain networks. Dialogues Clin. Neurosci. 15 (3), 247–262. https://doi.org/10.31887/DCNS.2013.15.3/osporns.

Sprugnoli, G., Rigolo, L., Faria, M., et al., 2022. Tumor BOLD connectivity profile correlates with glioma patients' survival. Neuro-Oncol. Adv. 4 (1) https://doi.org/10.1093/noajnl/vdac153 vdac153.

Stupp, R., Hegi, M.E., Mason, W.P., et al., 2009. Effects of radiotherapy with concomitant and adjuvant temozolomide versus radiotherapy alone on survival in glioblastoma in a randomised phase III study: 5-year analysis of the EORTC-NCIC trial. Lancet Oncol. 10 (5), 459–466. https://doi.org/10.1016/S1470-2045(09)70025-7.

Talozzi, L., Forkel, S.J., Pacella, V., et al., 2023. Latent disconnectome prediction of long-term cognitive-behavioural symptoms in stroke. Brain 146 (5), 1963–1978. https://doi.org/10.1093/brain/awad013.

Tan, A.C., Ashley, D.M., López, G.Y., Malinzak, M., Friedman, H.S., Khasraw, M., 2020. Management of glioblastoma: state of the art and future directions. CA A Cancer J Clin. 70 (4), 299–312. https://doi.org/10.3322/caac.21613.

Warren, J.D., Rohrer, J.D., Hardy, J., 2012. Disintegrating brain networks: from syndromes to molecular nexopathies. Neuron 73 (6), 1060–1062. https://doi.org/10.1016/j.neuron.2012.03.006.

Wei, Y., Li, C., Cui, Z., et al., 2023. Structural connectome quantifies tumour invasion and predicts survival in glioblastoma patients. Brain 146 (4), 1714–1727. https://doi.org/10.1093/brain/awac360.

Zhang, N., Xia, M., Qiu, T., et al., 2018. Reorganization of cerebro-cerebellar circuit in patients with left hemispheric gliomas involving language network: a combined structural and resting-state functional MRI study. Hum. Brain Mapp. 39 (12), 4802–4819. https://doi.org/10.1002/hbm.24324.